Journal of Sedimentary Research

Journal of Sedimentary Research, 2015, v. 85, 715–728
Research Article
DOI: http://dx.doi.org/10.2110/jsr.2015.42

FLUVIAL–EOLIAN INTERACTIONS IN SEDIMENT ROUTING AND SEDIMENTARY SIGNAL BUFFERING: AN EXAMPLE FROM THE INDUS BASIN AND THAR DESERT

AMY E. EAST,[1] PETER D. CLIFT,[2] ANDREW CARTER,[3] ANWAR ALIZAI,[4] AND SAM VANLANINGHAM[5]

[1]*U.S. Geological Survey, 400 Natural Bridges Drive, Santa Cruz, California 95060, U.S.A.*
[2]*Department of Geology and Geophysics, Louisiana State University, Baton Rouge, Louisiana 70803, U.S.A.*
[3]*Department of Earth and Planetary Sciences, Birkbeck College, University of London, Malet Street, London WC1E 7HX, U.K.*
[4]*Geological Survey of Pakistan, ST-17/2, Gulistan-e-Jauhar, Karachi, Pakistan*
[5]*Oregon State University, Cascades Campus, 2600 NW College Way, Bend, Oregon 97701, U.S.A.*
e-mail: aeast@usgs.gov

ABSTRACT: **Sediment production and its subsequent preservation in the marine stratigraphic record offshore of large rivers are linked by complex sediment-transfer systems. To interpret the stratigraphic record it is critical to understand how environmental signals transfer from sedimentary source regions to depositional sinks, and in particular to understand the role of buffering in obscuring climatic or tectonic signals. In dryland regions, signal buffering can include sediment cycling through linked fluvial and eolian systems. We investigate sediment-routing connectivity between the Indus River and the Thar Desert, where fluvial and eolian systems exchanged sediment over large spatial scales (hundreds of kilometers). Summer monsoon winds recycle sediment from the lower Indus River and delta northeastward, i.e., downwind and upstream, into the desert. Far-field eolian recycling of Indus sediment is important enough to control sediment provenance at the downwind end of the desert substantially, although the proportion of Indus sediment of various ages varies regionally within the desert; dune sands in the northwestern Thar Desert resemble the late Holocene–Recent Indus delta, requiring short transport and reworking times. On smaller spatial scales (1–10 m) along fluvial channels in the northern Thar Desert, there is also stratigraphic evidence of fluvial and eolian sediment reworking from local rivers. In terms of sediment volume, we estimate that the Thar Desert could be a more substantial sedimentary store than all other known buffer regions in the Indus basin combined. Thus, since the mid-Holocene, when the desert expanded as the summer monsoon rainfall decreased, fluvial–eolian recycling has been an important but little recognized process buffering sediment flux to the ocean. Similar fluvial–eolian connectivity likely also affects sediment routing and signal transfer in other dryland regions globally.**

INTRODUCTION

During passage from source areas to long-term depositional sinks, a fraction of the sediment in transport in a river is extracted and stored at least temporarily, resulting in net sediment loss from the transfer system (e.g., Trimble 1983; Dunne et al. 1998; Petter et al. 2013). Stored sediment is later released and mixed with new river sediment to generate a potentially complicated sedimentary signal in the depocenter, especially those of large drainage basins. In this manner, erosional pulses caused by climatic change or tectonic events may be "buffered," and any signals resulting from changes in sediment flux may be diffused or entirely obscured in the downstream sedimentary record. The transmission of sediment-flux signals is a function of (1) transport efficiency within the sediment-transfer system, and (2) sediment extraction (long-term sequestration of sediment in a net-aggradational system).

The efficiency with which rivers transfer and export sediment depends on the relationship between sediment supply and the ability of a landscape system to export sediment. Alluvial rivers, in particular, limit the efficiency of watershed sediment export, buffering the transmission of environmental signals by storing sediment in overbank and floodplain deposits (Castelltort and Van den Driessche 2003; Simpson and Castelltort 2012; Armitage et al. 2013; Pizzuto 2014). As a result, environmental perturbations (and resulting changes in sediment flux) on time scales shorter than the time needed for downstream signal propagation may not be evident in the stratigraphic record of the ultimate depositional sink. The longer the transport pathway of an alluvial system, the less effectively it may transmit short-lived environmental signals, resulting in a greater buffering effect (Castelltort and Van den Driessche 2003).

Signal buffering has been most intensively studied and modeled for alluvial rivers, but it is less well understood in other sedimentary systems. Accommodation space on low-gradient coastal plains, deltas, and continental shelves can impart additional buffering effects, though without necessarily erasing all short-term climatic signals from the downstream stratigraphic record (Goodbred 2003; Clift et al. 2008; Wolinsky et al. 2010; Forzoni et al. 2014). Quaternary valley fill and mass-wasting deposits near mountainous source areas can be important sediment stores as well (Blöthe and Korup 2013; Clift and Giosan 2014). In dryland (arid and semiarid) regions sediment routing includes seldom-studied interactions between fluvial and eolian processes that are likely to introduce additional complexity (e.g., Bullard and Livingstone 2002; Belnap et al. 2011). Eolian processes have not been considered explicitly in previous assessments of source-to-sink sediment routing, to our

Published Online: June 2015
 1527-1404/15/085-715/$03.00

knowledge. A recent synthesis of connectivity in sediment-transfer systems (Bracken et al. 2015) mentioned possible contributions of glacial, mass-wasting, and eolian processes, but focused almost exclusively on sediment movement over hillslopes, between hillslopes and alluvial channels, and within channels. To represent connectivity in sediment routing comprehensively, all transport processes must be considered (Bracken et al. 2015), and in dryland regions that requires assessing the role of eolian processes.

Eolian deposits are both sources and sinks of fluvial sediment in arid and semiarid lands (e.g., Ramsey et al. 1999; Bullard and Livingstone 2002; Prins et al. 2009; Roskin et al. 2014). Fluvially sourced eolian dunes form as the wind reworks fluvial sediment into source-bordering dunes along the river margin that can feed dune fields progressively farther downwind of the river (Bullard and McTainsh 2003; Han et al. 2007; Gibling et al. 2008; Amit et al. 2011; Draut 2012). Wind can carry sediment hundreds of kilometers downwind from river channels, deltas, and continental-shelf deposits exposed during times of low sea level (Muhs et al. 2003; Amit et al. 2011), in some cases moving sediment back toward its source area. As a result, large dune fields such as the Thar Desert (India and Pakistan; Fig. 1A) have substantial potential to buffer or delay sediment movement from source areas toward the ocean.

Despite their potential to disrupt source-to-sink transport, links between fluvial and eolian processes are not widely recognized as interrupting environmental-signal transfer. This study synthesizes new and previously published stratigraphic and sediment-provenance data, and quantifies provenance relations between Thar Desert sand samples and fluvial sediment upwind and downwind, to evaluate recycling of sand between the Indus River and the Thar Desert over Holocene time. We infer that fluvial–eolian sediment recycling likely constitutes a major buffer, with the desert being probably the largest storage zone in the Indus sediment-routing system. We propose that similar fluvial–eolian connectivity probably affects signal transfer in other dryland regions, but that its importance has been little recognized.

REGIONAL SETTING AND PREVIOUS WORK

The Indus River is the only major river draining the western Himalaya and Karakoram ranges (Fig. 1). It delivers sediment to the Arabian Sea, building the world's second-largest submarine fan. The Indus has a long history of drainage evolution, including, in Holocene time, abandonment of the Yamuna River course in the northeastern Punjabi floodplain owing to headwater capture (Valdiya 2002; Saini et al. 2009; Clift et al. 2012) and the drying up of the Ghaggar–Hakra River tributary after ~ 4 ka (Giosan et al. 2012). Fluvial sediment recycling in the Indus system is apparent from incision of rivers into the northern portion of the floodplains, adjacent to the Himalaya (whereas the southern portion of the Indus floodplain adjacent to the delta continues to aggrade); Clift and Giosan (2014) estimated that incision and reworking of sediment from the northern floodplains accounts for 21–23% of the flux into the coastal zone since the last glacial maximum (LGM), totaling> 900 km^3. Rivers have incised into the northern parts of the Punjabi floodplains at the northern (downwind) side of the Thar Desert since the early Holocene (Giosan et al. 2012), reworking sediment 10 ka and older. Sediment sequestration in Himalayan valley fill and mass-wasting deposits also introduces additional sediment residence times of 1–100 kyr in some regions of the Indus and Ganges–Brahmaputra River systems (Blöthe and Korup 2013).

The Thar Desert dates from at least mid-Pleistocene time (Wasson et al. 1983; Glennie et al. 2002; Singhvi et al. 2010). The southwest summer monsoon is the prevailing influence on wind and rainfall in this region, with eolian sediment transport dominantly from southwest toward northeast (Fig. 1); summer months typically include dry, windy conditions, commonly with dust storms, followed by late-summer rain (Singhvi et al. 2010). Winter winds play a substantially lesser role in sand transport and dune formation, and their principal effects are restricted to the northern Thar Desert (Kar 1993). The desert is bounded to the west by the Indus River and its eastern tributaries, including the Sutlej River immediately to the north.

Several studies have described and dated sedimentary profiles from the Thar Desert and neighboring fluvial environments, revealing the timing of sediment storage and erosion. These show that the Thar Desert expanded after the LGM, during phases of strengthened summer monsoon (Singhvi et al. 2010). However, the desert also continued its advance westward during weakening of the summer monsoon starting after ~ 8 ka (e.g., Gupta et al. 2003). An approximately 200-kyr record from the east-central Thar Desert of sediment composition, mineralogy, and optically stimulated luminescence (OSL) and thermoluminescence (TL) ages showed at least 12 cycles of eolian sedimentation, alternating with geomorphic stability accompanied by soil formation (Singhvi et al. 2010). Several sedimentary profiles with relevance for dating desert evolution and determining provenance are reproduced in Figure 2 (Singhvi and Kar 2004; Clift et al. 2008; Alizai et al. 2011a; Giosan et al. 2012), demonstrating the westward expansion of the desert during Holocene time. Singhvi and Kar (2004) inferred rapid sediment accumulation in the central part of the desert through the Holocene—for example, 7 m of accretion since the LGM at Chamu (Fig. 2). On the western edge of the desert, e.g., in the Nara Valley, the dunes have advanced over the floodplains more recently. Dunes yield ages ranging from ~ 1.42 ka at Yazman to 0.44 ka at Section MGJ-5, on the northern side of the desert (Fig. 2; Giosan et al. 2012). In other locations the age of dune advance is interpreted to be necessarily younger than the underlying fluvial sediments, with the general trend indicating desert expansion after 4.8 ka (Durcan et al. 2010), during a phase of weakening monsoon rainfall (Enzel et al. 1999; Fleitmann et al. 2003; Gupta et al. 2003). At Chundkho, in the Nara region (Fig. 2), silty loess deposits also indicate dry, windy conditions between 7.0 and 4.8 ka, after which time sand dunes buried the loess.

Connectivity between fluvial and eolian sedimentary systems in the Indus watershed and Thar Desert—with the desert acting as both source and sink for fluvial material—has been documented to varying degrees by the aforementioned stratigraphic studies and some provenance analyses. Earlier stratigraphic studies demonstrated local fluvial–eolian coupling of dune sediment and fluvial material in the Thar Desert, river channels, and floodplains (Singhvi and Kar 2004; Clift et al. 2012; Giosan et al. 2012; Fig. 2). Fluvial erosion of eolian dunes along the Nara River valley (likely a former south-flowing course or distributary of the Indus River), as well

→

FIG. 1.—**A)** Regional context of the Indus River catchment, major tributaries, the Thar Desert, and locations discussed in the text. Boxes show areas covered in Parts B and C. The Punjabi floodplains comprise the Sutlej and Ghaggar–Hakra (G-H) Rivers and other adjacent channels. Image courtesy of Google Earth. The site at Tatapani included both a pre-existing zircon U–Pb analysis (Alizai et al. 2011a) and newly analyzed Nd isotope data for the Sutlej River (this study). **B)** False-color image of a portion of the northwestern downwind end of the Thar Desert and Sutlej River course, in Cholistan. **C)** False-color image of the Nara Valley, western Thar Desert. Eolian dunes are shown in pink; prevailing wind direction is toward north-northeast. Images in Parts B and C courtesy of NASA Worldwind. Green circles, sample locations of Nd isotope data from Tripathi et al. (2004); yellow circles, sample locations of new Nd isotope data (this study); blue squares, sample locations for U-Pb zircon data of Clift et al. (2008) and Alizai et al. (2011b); pink squares, sample locations for new U-Pb zircon data (this study); white circles, boreholes and stratigraphic sections shown in Figure 2 that are not already represented by one of the aforementioned symbols.

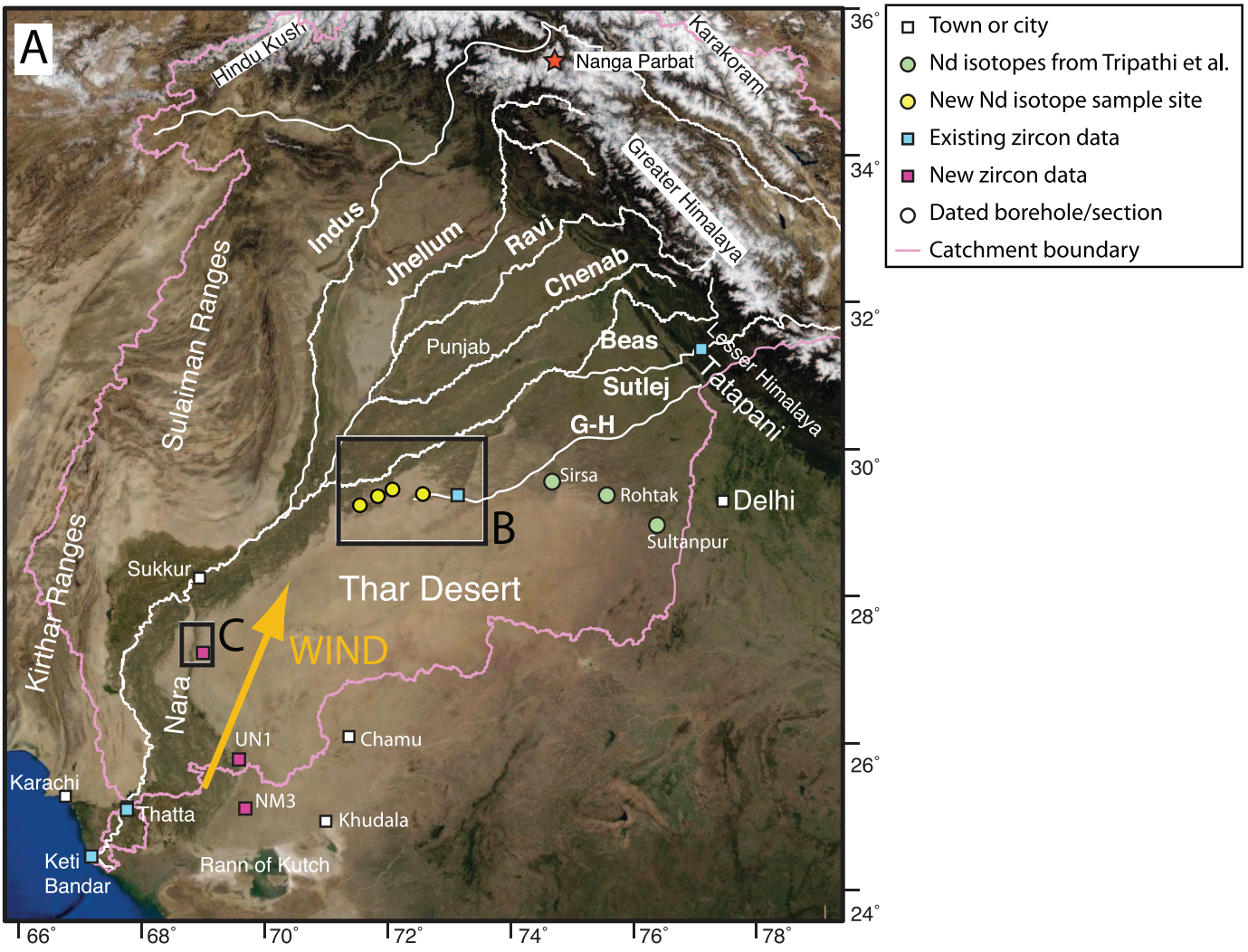
A
Hindu Kush
Nanga Parbat
Karakoram
Greater Himalaya
Indus
Jhellum
Ravi
Chenab
Punjab
Beas
Sutlej
G-H
Lesser Himalaya
Tatapani
Sulaiman Ranges
Kirthar Ranges
Nara
Sirsa
Rohtak
Delhi
Sultanpur
Sukkur
B
C
Thar Desert
WIND
UN1
Chamu
Karachi
Thatta
NM3
Khudala
Keti Bandar
Rann of Kutch
Town or city
Nd isotopes from Tripathi et al.
New Nd isotope sample site
Existing zircon data
New zircon data
Dated borehole/section
Catchment boundary
36°
34°
32°
30°
28°
26°
24°
66°
68°
70°
72°
74°
76°
78°

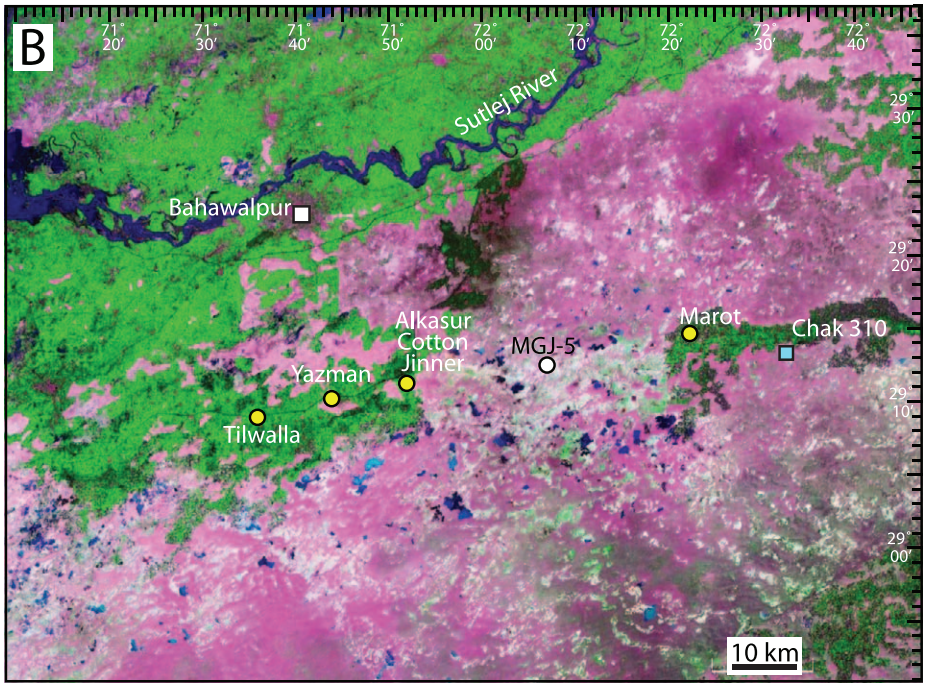
B
Sutlej River
Bahawalpur
Alkasur Cotton Jinner
MGJ-5
Yazman
Tilwalla
Marot
Chak 310
10 km

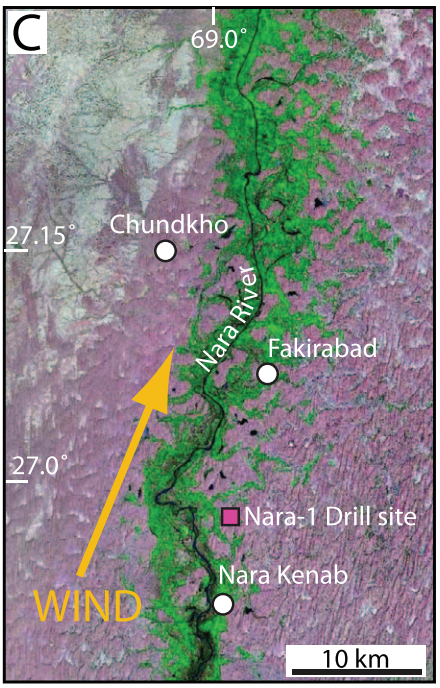
C
69.0°
27.15°
27.0°
Chundkho
Nara River
Fakirabad
Nara-1 Drill site
Nara Kenab
WIND
10 km

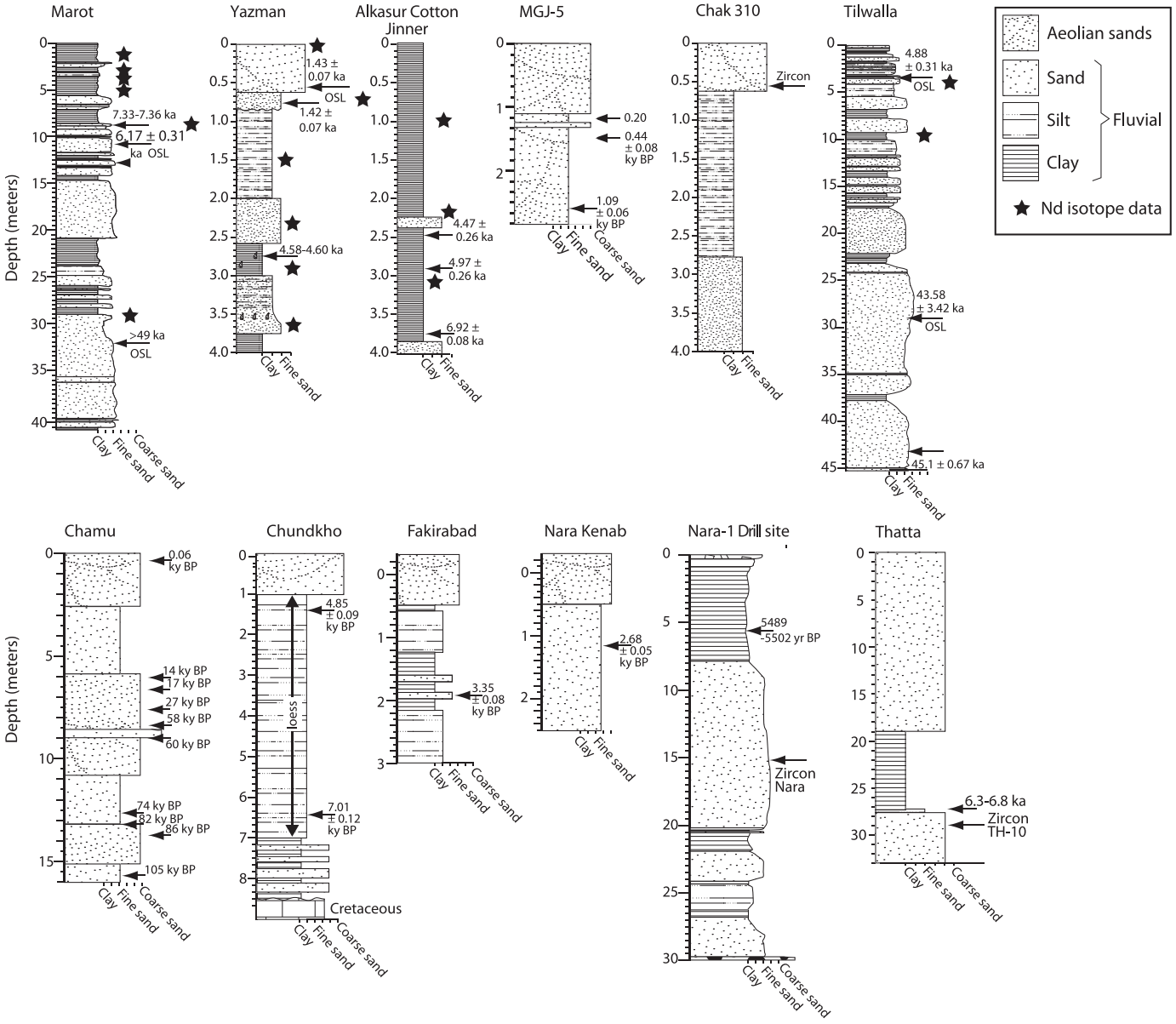

FIG. 2.—Sedimentary profiles from the Thar Desert, Nara Valley, Sutlej River valley, and lower Indus River and delta. Section from Chamu is from Singhvi and Kar (2004). Section from Thatta is from Clift et al. (2008). Sections from Marot, Yazman, Fakirabad, and Nara drill site are from Alizai et al. (2011a). Section from Tilwalla is from Clift et al. (2012). Sections from Alkasur Cotton Jinner, MGJ-5, and Nara Kenab are from Giosan et al. (2012). Section from Chak 310, this study (zircon sample analyzed by Alizai et al. 2011b). Section from Chundkho, this study. See Figure 1 for locations. Ages indicated by sedimentary horizons were determined by optically stimulated luminescence (OSL) where indicated; other ages were determined by accelerator mass spectrometry (AMS) radiocarbon dating of organic material and mollusk shells at the National Ocean Sciences Accelerator Mass Spectrometry Facility (NOSAMS) at the Woods Hole Oceanographic Institution, Massachusetts, USA (http://nosams.whoi.edu); dates were converted to calendar ages using the IntCal04 calibration dataset (Reimer et al. 2004) for plant matter and Calib 5.0.1 software for mollusk shells (Stuiver et al. 1998).

as along the former course of the Ghaggar–Hakra River, is clear from satellite images (Fig. 1B, C). That the Indus delta region serves as a sediment source for the Thar Desert is evident from foraminifera tests in the central and northeastern Thar Desert sand that are derived from shallow marine regions (Kameswara Rao et al. 1989). The importance of Thar Desert sediment sources originating in the lower Indus River and delta is also apparent from the dominant orientations of eolian dunes throughout the desert—transverse, parabolic, and linear forms indicate the prevalence of north-northeastward eolian sediment transport (Fig. 1A, C).

Initial sediment-provenance analyses have supported the concept that eolian recycling of fluvial sediment could be a major influence in Indus sediment routing. As part of a study of Indus-basin drainage evolution since the Pleistocene, Alizai et al. (2011a, 2011b) demonstrated that Pb isotopes from detrital K-feldspar grains, as well as then-available U-Pb zircon and Nd isotopic data, showed similarity between the lower reaches of the mainstem Indus River (i.e., downstream of the last major tributary confluence) and the downwind (northern) Thar Desert. Here, we expand substantially upon previous provenance analyses by presenting new U-Pb zircon and Nd isotopic data from the Thar Desert and Indus basin.

TABLE 1.—*Sediment samples from which U-Pb zircon data are available for tracing provenance history among the Thar Desert, Indus River, and adjacent tributary basins (Sutlej River and Nara Valley).*

Sample	Location	Latitude	Longitude	Sediment Type	Data Source
Thar Chak-310	Thar desert, downwind end	29.210867	72.484900	Eolian dune	Alizai et al. (2011)
Thar UN1	Thar desert, upwind end, near Umerkot town	25.369611	69.732722	Eolian dune	This study
Thar NM3	Thar desert, upwind end, near Mithi town	24.858972	69.726250	Eolian dune	This study
Sutlej River	Sutlej River at Tatapani	31.000000	76.550000	Fluvial (modern)	Alizai et al. (2011a)
Nara	Nara Valley drill site (Nara-1), 15 m depth	26.976017	68.990900	Borehole sample, fluvial sand	This study
Indus River, modern	Modern Indus delta at Thatta	24.618817	68.049500	Fluvial (modern)	Clift et al. (2004)
Indus 7 ka TH-10	Indus delta at Thatta, 7 ka, 30 m depth	24.702306	67.990972	Borehole sample, fluvial sand	Clift et al. (2008)
Indus LGM KB-41-5	Indus delta at Keti Bandar	24.152400	67.515533	Fluvial (modern)	Clift et al. (2008)

We use the new and previously existing data together to quantify provenance relations among the fluvial and eolian components of the Thar–Indus system. We use the resulting provenance relations to evaluate how substantially fluvial–eolian connectivity over large spatial scales may have buffered sediment delivery from the Indus River system to the ocean.

PROVENANCE ANALYSIS: DATA SOURCES AND METHODS

In order to assess the importance of various possible sediment sources contributing to eolian sand in the Thar Desert, and thus the importance of eolian supply from the lower Indus River and delta, we compiled available U-Pb zircon and Nd-isotope provenance data from Thar Desert samples and surrounding fluvial environments. The latter include the lower Indus River and delta spanning the time since the LGM, the Nara Valley, and the southern part of the Punjabi floodplains (the Sutlej River and the downstream end of the former Ghaggar–Hakra River course, which border the Thar Desert on the downwind side; Fig. 1).

In addition to three new U-Pb zircon age spectra described below, we refer to the U-Pb zircon provenance work of Clift et al. (2004, 2008) and Alizai et al. (2011a, 2011b), utilizing age spectra from: (1) an eolian dune sand sample at site Chak-310 (Alizai et al. 2011b); (2) a sample of modern fluvial sand from the Sutlej River at Tatapani close to where this river leaves the Himalayan source area, in the downstream-most mountainous terrain of the Sutlej basin (Alizai et al. 2011a; location in Fig. 1A); (3) a fluvial sediment sample from a depth of 118 m in a borehole on the Indus delta at Keti Bundar dated to the LGM (age loosely constrained to between 28.7 and 20 ka; Clift et al. 2008); (4) an Indus River fluvial sand sample from a depth of 30 m in a borehole at Thatta (sample TH-10), dated to 7 ka (Clift et al. 2008); and (5) a sample of modern lower Indus River fluvial sand collected in the active river channel 200 m away from the Thatta borehole site (Clift et al. 2004).

Samples of eolian dune sand were collected for U-Pb detrital-zircon analysis from two locations (UN1 and NM3) near the upwind, southern extent of the Thar Desert (Fig. 1A). We also analyzed the U-Pb zircon age spectrum from a fluvial sand sample collected at a depth of 15 m in a borehole in the Nara Valley (Nara-1 drill site, Fig. 1C) from which the full sedimentary profile (Fig. 2) was described by Alizai et al. (2011b) and Giosan et al. (2012). Zircon grains were extracted from each of these three samples (UN1, NM3, and Nara) and their U-Pb age spectra were determined from polished grain mounts by laser ablation inductively coupled plasma mass spectrometry (LA-ICP-MS) at University College London. This facility employs a New Wave 193 nm aperture-imaged, frequency-quintupled laser ablation system coupled to an Agilent 7700 quadrupole-based ICP-MS. The laser was set up to produce an energy density of ca 2.5 J/cm^2 at a repetition rate of 10 Hz. Repeated measurements of external zircon standard PLESOVIC (TIMS reference age 337.13 ± 0.37 Ma; Sláma et al. 2008) and NIST 612 silicate glass (Pearce et al. 1997) were used to correct for instrumental mass bias and depth-dependent inter-element fractionation of Pb, Th, and U. Temora (Black et al. 2003) and 91500 (Wiedenbeck et al. 2004) zircon were used as secondary age standards. Data were filtered using standard discordance tests with a 15% cutoff. We used the $^{206}Pb/^{238}U$ ratio to determine ages where <1000 Ma, and the $^{207}Pb/^{206}Pb$ ratio for older grains. Data were processed using GLITTER 4.4 data-reduction software. Time-resolved signals that record evolving isotopic ratios with depth in each crystal enabled filtering to remove spurious signals owing to overgrowth boundaries, inclusions, or fractures. Data were then filtered using standard discordance tests and applying a 10% cutoff. Between 96 and 186 grain ages were measured in each sample, in order to generate a statistically meaningful data set (Vermeesch 2004).

We compiled new and previously published analyses to examine Nd isotopic provenance affinity as well, because this isotopic system is known to be resistant to the effects of chemical weathering and has a proven record as a source discriminant in the Indus basin (Clift et al. 2008, 2012). Furthermore, this method allows comparison with other dune sands from the northeastern end of the Thar Desert, from which we refer to earlier analyses of Tripathi et al. (2004), focusing on their eolian sand samples (n = 9) from three locations in the northeastern Thar Desert (Sirsa, Rohtak, and Sultanpur; Fig. 1A) and fluvial samples (n = 6) from the modern Sutlej River (Tripathi et al. 2004). We also utilized Nd isotopic analyses from modern (n = 1), Holocene (n = 16), and LGM-age (n = 1) fluvial sediment samples from boreholes along the lower Indus River and delta (Clift et al. 2002, 2008).

Nd isotopic compositions were analyzed for this study in 18 sediment samples, including 16 fluvial samples from borehole profiles in floodplain locations at Tilwalla, Yazman, Alkasur Cotton Jinnar, and Marot (in the Cholistan region of Pakistan, nearest the Sutlej River and former Ghaggar–Hakra course, Fig. 1B; locations and sedimentary horizons are shown in Fig. 2), one sample of modern Sutlej River sediment at Tatapani (Fig. 1A), and one surface sample of eolian sediment at Yazman. Nd isotopic content was determined for the organic- and carbonate-free sediment dissolved in 8 N HF for 24 hr and converted to chlorides. The material was passed through cation-exchange and chromatography columns to separate Nd. Samples were analyzed in dynamic mode on a Nu® Instruments multi-collector ICP-MS at Oregon State University, and corrected for instrument bias by bracketing each sample with a J-Ndi standard (Tanaka et al. 2000) for which reproducibility was 0.000024 (2σ, n = 57). Nd isotopic values are discussed in terms of ε_{Nd} (DePaolo and Wasserburg 1976), which is the $^{143}Nd/^{144}Nd$ ratio calculated relative to the Chondritic Uniform Reservoir (CHUR) standard.

RESULTS

U-Pb zircon age spectra from the three eolian and five fluvial samples considered (Table 1; analyses from new samples available from JSR's Data Archive, see Supplemental Material) show various proportions of zircon grains of different ages. We used these ages to infer likely

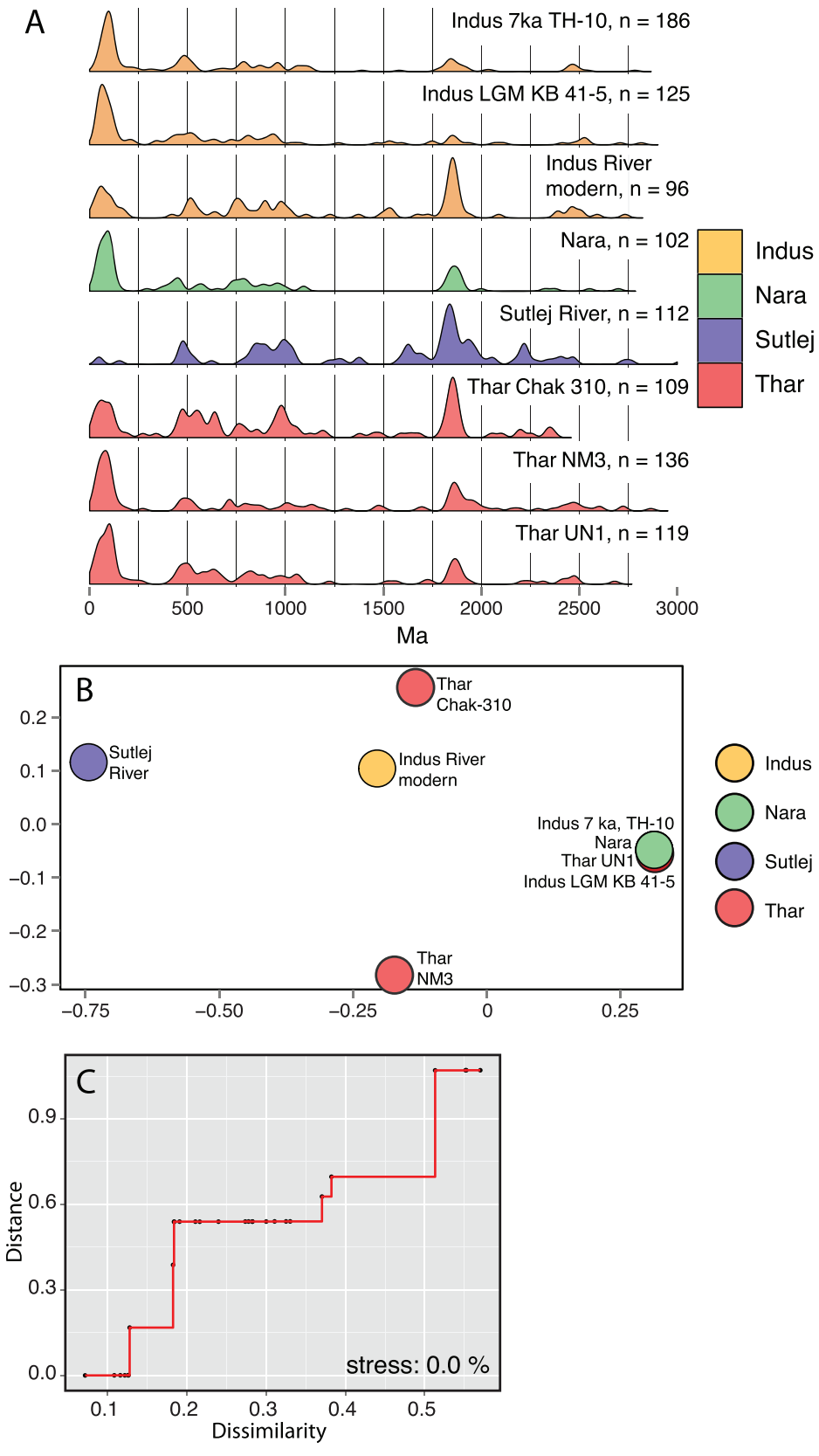

FIG. 3.—Results of detrital-zircon U-Pb age-spectra comparisons. **A)** Kernel density estimation (KDE) plots for U-Pb ages in detrital zircon grains from the Thar Desert, the modern Indus and Sutlej rivers, the Nara River before 5.5 ka, as well as the Indus River mouth at 7 ka and at ~ 20 ka. Data sources as shown in Table 1. Characteristic age ranges are shown for the Karakoram source terrane (Le Fort et al. 1983; Parrish and Tirrul 1989; Schärer et al. 1990; Searle et al. 1990; Fraser et al. 2001), Greater Himalayas (Noble and Searle 1995; Hodges et al. 1996; Parrish and Hodges 1996; DeCelles et al. 2000; Gehrels et al. 2006), and Lesser Himalayas (Parrish and Hodges 1996; DeCelles et al. 2000). **B)** Multidimensional scaling (MDS) mapping (cf. Vermeesch 2013) group samples with similar age spectra, and separates samples with different spectra. Values on the axes are units of space. **C)** "Shepard diagram" provides a graphical assessment of MDS model fit, which is perfect in this case; see text for further description.

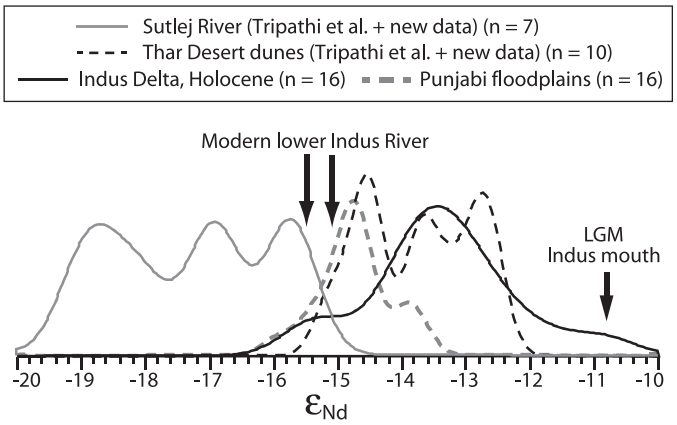

FIG. 4.—Kernel density estimation (KDE) plot of ε_{Nd} values for the Thar Desert and other possible sediment sources. Thar Desert eolian sand data and Sutlej River sand data from Tripathi et al. (2004). Holocene and last glacial maximum (LGM) lower Indus delta data are from sand samples in boreholes studied by Clift et al. (2008), largely at Keti Bundar (location in Fig. 1A). Modern lower Indus River sand value from Thatta (–15.5) and just below the confluence of the Indus and Sutlej rivers (–15.1) are from Clift et al. (2002). Punjabi floodplains data, this study.

derivation from Lesser Himalaya, Greater Himalaya, and Karakoram source terranes, as expected for sediment in the Indus basin (Fig. 3A). Grains younger than 300 Ma are not unique to the Karakoram range, but earlier studies have shown that this is the most important source of zircons of this age to the Indus River (Alizai et al. 2011b). Likewise, grains dating to 1700–2000 Ma are found in the Greater as well as the Lesser Himalaya, but are statistically more common in the Lesser Himalaya, such that modern rivers that drain the Lesser Himalaya tend to be much richer in 1700–2000 Ma grains than are rivers that drain just the Greater Himalaya (DeCelles et al. 2000).

Although a visual comparison can be informative as to the similarity among age spectra of different samples (Fig. 3A), we quantified their similarity more rigorously by using the statistical effect size of the Kolmogorov–Smirnov (KS) test and then plotting the results using a standard statistical method known as multidimensional scaling (MDS; see Vermeesch 2013) to produce a map (Fig. 3B) of the pattern of similarity or dissimilarity among the age spectra. The values on the axes of non-metric MDS plots simply give the rank order of similarity. This serves to group samples with similar age spectra and pull apart samples with different spectra. The accompanying Shepard plot (Fig. 3C) represents how well the MDS "fitted distances" (distances measured with a ruler) match the true (KS) distances; the stepped line represents a transformation of the input data. If all of the reproduced distances fall onto the stepped line, then the rank ordering of distances (or similarities) has been perfectly reproduced. The stress value is a measure of the overall goodness of fit, whereby the higher the stress value the poorer the fit. Essentially, the quality of the model fit in this case is perfect. These statistical comparisons indicate that: (1) the three Thar Desert eolian sand samples differ significantly from each other; (2) eolian sample Chak-310, from the downwind end of the Thar Desert in Cholistan, is similar to the modern Indus River fluvial sediment at Thatta; (3) the eolian sample UN1, from the upwind end of the desert, is statistically indistinguishable from fluvial samples from the Nara Valley, the lower Indus River–delta at the LGM, and the lower Indus River at 7 ka; (4) the eolian sample NM3 is statistically different from any other sample, but bears closest resemblance to the modern Indus River at Thatta; and (5) the Sutlej River sample shows an age spectrum unlike that of any other sample.

The Nd isotopic data show similarity between ε_{Nd} values of the Indus River at various time intervals and eolian dune sand at the downwind end of the Thar Desert (Fig. 4; new analyses shown in Table 2). The ε_{Nd} range for 10 Thar Desert samples (–12 to –15.6) largely overlaps with values from the modern lower Indus River and delta (this study and Tripathi et al. 2004). The dune samples also overlap with the values for Holocene-age Indus delta sediment (Fig. 4; Clift et al. 2008), although some dunes from the northeastern desert region are more negative in ε_{Nd} than most delta samples. The 16 samples analyzed from the southern Punjabi floodplain region of the Sutlej and Ghaggar–Hakra rivers (Fig. 1B) show ε_{Nd} values that overlap well with those of the modern lower Indus River, the more negative end of the Holocene Indus delta, and the more negative end of the Thar Desert samples (Fig. 4). Notably, all seven samples from the Sutlej River (farther upstream than the Punjabi floodplains localities) show ε_{Nd} values that are substantially lower than any obtained from the Indus River or Thar Desert samples (Fig. 4), even though the Sutlej River occurs in such proximity to the downwind end of the Thar Desert.

DISCUSSION

To evaluate the role of eolian recycling in Indus basin sediment routing, we can use provenance analysis to identify the contribution of local and far-field sediment sources to Thar Desert eolian sand. Although eolian dunes at the downwind, northern end of the Thar Desert might be expected to receive most sediment from local rivers rather than from the Indus River, given the relative proximity of each, sand at the downwind end of the desert instead has greater provenance affinity with the lower Indus River and delta sediments (hundreds of kilometers upwind). There is remarkable similarity between the modern lower Indus River and delta region and recent eolian dune sand even far downwind (estimated to have been deposited no earlier than 1.4 ka, based on the age of basal eolian dune sand at Yazman; Fig. 2), whereas the dune sand differs significantly from that of more local river sources on the southern Punjabi floodplains.

The apparent dominance of Thar Desert dune sediment from sources in the lower Indus River and delta region, based on U-Pb age spectra and ε_{Nd} patterns (Figs. 3, 4) is in agreement with earlier findings that used Pb isotope analyses as a provenance tool (Alizai et al. 2011a). At Yazman and Site MGJ-5 (Fig. 1), Pb isotopes from K-feldspar grains (Alizai et al. 2011a) showed little affinity between the eolian sands and the adjacent Sutlej River. Instead the dunes comprised feldspar grains with high $^{207}Pb/^{204}Pb$ and $^{206}Pb/^{204}Pb$ values and zircon grains with U-Pb crystallization ages of <100 Ma, which are typical of erosion of the Nanga Parbat metamorphic massif and arc-type sources respectively, and thus an indicator of an origin within the mainstem Indus River, but not the Sutlej River. Direct reworking between the upper Indus mainstem and the desert can be ruled out on geomorphic grounds, requiring these Nanga Parbat-derived grains to have been transported fluvially to the lower reaches and then reworked northeastward by wind. Thus, we infer that far-field sediment sources in the lower mainstem Indus River dominate the provenance signal in the Thar Desert samples discussed here, and we attribute that dominance to wind transport. Although in some areas, bedrock outcrops in the Thar Desert also locally contribute some sediment to dunes (Wasson et al. 1983), visual field observations during this study suggested that bedrock sediment sources are important only over spatial scales of several dune lengths; bedrock sources were not observed at or immediately upwind of the Thar Desert sites sampled for this study.

Simple mixing calculations can indicate possible relative contributions to the Thar Desert samples of Indus sediment from various time intervals, or from the Sutlej River, if any. We consider mixing relations using the available U-Pb zircon age spectra and Nd isotopic data, attempting to reconcile the proportions of modern Indus River sediment, mid-Holocene Indus delta sediment, and Indus delta sediment of LGM age that

TABLE 2.—*Results of Nd isotopic analyses (presented as relative frequency of ε_{Nd} values), showing new and previously published data. New data include one measurement from the modern Sutlej River at Tatapani (sample S3), and 17 from the southern Punjabi floodplain region of the Sutlej and Ghaggar–Hakra river courses. Of the latter 17, Sample S4-081109-18 is eolian sediment, all others are fluvial.*

Sample	Location Name	Latitude	Longitude	Depth Subsurface (m)	$^{143}Nd/^{144}Nd$	Error (2σ)	ε_{Nd}
S3-Sutlej River, 20–63 μm	Tatapani	31°14'41.15"N	77° 5'24.21"E	0	0.511660	8.00E-06	**-19.07**
S9-CJ-4-1, 91–103 cm	Alkasur Cotton Jinner	29° 9'5.32"N	71°51'19.46"E	0.97	0.511886	1.28E-05	**-14.68**
S6-CJ-4-7, 233–240 cm, 20–63 μm	Alkasur Cotton Jinner	29° 9'5.32"N	71°51'19.46"E	2.37	0.511854	9.00E-06	**-15.29**
S10 CJ-4-10, 291–300 cm	Alkasur Cotton Jinner	29° 9'5.32"N	71°51'19.46"E	2.96	0.511897	1.20E-05	**-14.45**
S19 M1 0.27–0.30	Marot	29°12'47.76"N	72°20'28.38"E	0.29	0.511881	1.76E-05	**-14.76**
S20 M2A 1.93–1.95	Marot	29°12'47.76"N	72°20'28.38"E	1.94	0.511935	1.24E-05	**-13.72**
S13 M2A 2.59–2.64	Marot	29°12'47.76"N	72°20'28.38"E	2.61	0.511924	1.32E-05	**-13.92**
S14 M2B 3.0–3.02	Marot	29°12'47.76"N	72°20'28.38"E	3.01	0.511925	9.80E-06	**-13.91**
S15 M5A 8.95–8.97	Marot	29°12'47.76"N	72°20'28.38"E	8.96	0.511865	6.80E-06	**-15.07**
S16 M12A 29.88–29.90	Marot	29°12'47.76"N	72°20'28.38"E	29.89	0.511847	7.60E-06	**-15.42**
S17 T2 3.42–3.45	Tilwalla	29° 5'42.22"N	71°34'3.39"E	3.44	0.511878	7.00E-06	**-14.83**
S18 T4 9.18–9.20	Tilwalla	29° 5'42.22"N	71°34'3.39"E	9.19	0.511823	4.00E-06	**-15.90**
S4-081109-18, <63 μm	Yazman (eolian)	29° 7'23.16"N	71°46'10.08"E	0	0.511895	9.20E-06	**-14.50**
S8-081109-17, 20–63 μm	Yazman	29° 7'23.16"N	71°46'10.08"E	0.70	0.511880	1.46E-05	**-14.79**
S1-081109-16, 20–63 μm	Yazman	29° 7'23.16"N	71°46'10.08"E	1.50	0.511887	9.60E-06	**-14.65**
S5-081109-15, 20–63 μm	Yazman	29° 7'23.16"N	71°46'10.08"E	2.30	0.511881	1.20E-05	**-14.78**
S7-081109-14, 20–63 μm	Yazman	29° 7'23.16"N	71°46'10.08"E	2.90	0.511891	8.40E-06	**-14.56**
S11 081109-11, 20–63 μm	Yazman	29° 7'23.16"N	71°46'10.08"E	3.70	0.511880	1.04E-05	**-14.79**

compose the Thar Desert eolian samples at the downwind end of the desert. For the calculations that follow, we follow traditional detrital-zircon provenance techniques in assuming that the zircon populations are representative of the bulk siliciclastic content (e.g., Carter and Bristow 2001).

In order to estimate the possible contributions from different sources we consider the zircon age population split into the peaks seen in the KDE plots (Fig. 3) and attempt to reproduce the desert-sand zircon populations by mixing possible end members together. In particular, we focus on the relative sizes of the age populations in both the Indus delta sediment and the Thar Desert samples. We compare zircon grains in the following groups: 0–300 Ma, 300–750 Ma, 750–1200 Ma, and 1500–2300 Ma. Other grains are removed from this calculation and the total normalized to 100% in order to simplify our mixing estimate. The <300 Ma group is especially diagnostic because it is rare in the Sutlej River sample (3% of the total zircon population), more abundant in the modern Indus River at Thatta (~ 23%), and very common in the Indus delta at 7 ka (49%) and at the LGM (47%). Care needs to be taken concerning the grain sizes of the material analyzed. Recent work by Yang et al. (2012) that analyzed sediments from the mainstream and tributaries of the Yangtze River revealed that younger zircons were larger or more variable in size than were the older grains, implying a potential influence of hydrodynamic fractionation on zircon size and age. No specific grain-size information for our zircon samples was collected as part of this study, but, by inspection, fine sand dominated our data set. Yang et al. (2012) concluded that the 63–125 μm size fraction yielded almost the same age population as the bulk population of zircons.

Ideally, we would like to correct for the relative abundance of zircon grains in each particular end member. This has been done previously in other zircon budgeting studies that have used Zr concentration as a proxy for the relative abundance of zircon crystals in different sands (Amidon et al. 2005). If we were to take that approach, it would require assuming that the analyzed sample from each end member is representative of the average composition from the Indus River at each end-member time interval. However, this correction may not be very accurate depending on exactly where in the stream or delta the sample was collected. Hydrodynamic sorting may preferentially concentrate or dilute zircon in any particular sample relative to the average flux depending on where and when the sample is taken from the river channel. Although hydrodynamic sorting is unlikely to change the ages of the zircons sampled, it can result in significant variations in relative concentration over short time and length scales. Unless we know that the river sand is representative of the end member at the time of deposition, then making any type of correction will introduce additional uncertainties. In view of the large size of the drainage basins and therefore the unlikelihood that the source rocks are significantly different in total zircon concentration because of the diversity of source rocks in each subbasin, we do not to try to correct for Zr concentration because it is likely to add more uncertainty than it would resolve. In this study we estimate possible contributions by mixing together end members using the relative

TABLE 3.—*Percentages of different age groups in U-Pb zircon age spectra for Indus River end-member sediment sources from three time periods (LGM, 7 ka, and modern) considered in mixing calculations, together with relative abundance in three Thar Desert dune sand samples from which zircon data are available (NM3, UN1, and Chak-310). Also shown are Nd isotope compositions for the end members.*

Age groups (Ma)	Indus LGM	Indus 7 ka	Indus modern	Sutlej River	NM3	UN1	Chak 310
0–300	46.9	48.6	23.5	3.0	43.1	39.8	22.1
300–750	23.2	17.7	17.6	10.1	13.8	23.9	26.0
750–1250	19.5	20.0	22.4	27.3	15.5	17.7	23.1
1500–2300	10.4	13.7	36.5	59.6	27.6	18.6	28.8
	100	100	100	100	100	100	100
ε_{Nd}	–10.8	–13.5	–15.3	–19.0			

abundances of the different Indus River–delta age populations as measured by Clift et al. (2008) and Alizai et al. (2011b). It is not possible to reproduce the observed age spectra perfectly for the desert sands, so we particularly focused on diagnostic populations such as those <300 Ma, which are unique to the mainstem Indus River, as well as those dated at 1500–2300 Ma, which are also abundant in the Sutlej River (2011b). Because the Nd-isotope composition is known for each of these end members, it is possible to predict the Nd-isotope composition of the Thar Desert dune sand mixed in these proportions. Unfortunately, none of the eolian dune samples considered here has Nd data available, but we can compare the zircon-derived budget and its predicted Nd compositions with existing Nd data from dune sediment in the far northeastern part of the desert (Tripathi et al. 2004).

At the downwind end of the desert, sample Chak-310 contained 22% grains in the age range <300 Ma, consistent with derivation from the modern or recent Indus delta, which contains 23.5% of such grains. Any substantial mixing with older Indus delta sediment would result in much higher proportions for this age population. Conversely, receiving sediment from the Sutlej River, which has virtually no zircon grains <300 Ma, would substantially reduce the proportion of this age group in Thar Desert sediment. The desert sand at site Chak-310 has a significant proportion of 1500–2300 Ma grains, consistent with derivation from the modern Indus delta. Grains of that age are also abundant in the Sutlej River, but because the latter lacks zircon grains <300 Ma, from a simple mixing calculation we estimate that the Chak-310 location contains as much as 90% material sourced from the modern lower Indus River, 0–10% sourced from Holocene (7 ka) Indus delta sediment, and 0–10% from locally derived Sutlej River sediment. Such proportions derived from the U-Pb zircon ages agree well with a similar mixing calculation performed using ε_{Nd} values; at Yazman, Cholistan, an ε_{Nd} value of –14.5 (Table 2) is consistent with having mixed modern lower Indus River sediment (average ε_{Nd} –15.3), Holocene Indus delta sediment (average ε_{Nd} –13.5), and Sutlej River sediment (average ε_{Nd} –17.5) in those proportions.

At the upwind side of the Thar Desert, samples NM3 and UN1 contain 43% and 40% grains in the <300 Ma age range, respectively (Table 3), suggesting that these locations were influenced largely by Indus-delta sediment sources ranging in age from LGM to mid-Holocene. Contribution of modern Indus sediment likely occurred also, although there is evidently a dominance of mid-Holocene Indus sediment at location UN1. For example, mixing calculations indicate that the zircon age spectrum for UN1 could result from 55% mid-Holocene (7 ka) Indus sediment, 35% from the modern lower Indus River and delta, and only 10% from the LGM delta, a combination that predicts 40% grains <300 Ma (Fig. 5; Table 3). The zircon age spectrum from sample NM3 indicates proportions of 7 ka, modern, and LGM Indus delta sediment of 64, 21, and 15%, respectively (Fig. 5).

Fluvial sands from the Nara Valley borehole that were deposited just before ~ 5.5 ka show abundant <300 Ma zircon grains (45% of the total) and some 1500–2300 Ma grains (19%), and the Nara sample zircon age spectrum is statistically indistinguishable from that of UN1 (which contains 40% <300 Ma and 19% 1500–2300 Ma grains), suggesting interaction between mainstem Indus and Thar Desert sediment at the upwind side of the desert (i.e., from Nara Valley to UN1) starting between 7.0 and 5.5 ka (Clift et al. 2012). Because the samples UN1 and NM3 were collected on the surfaces of presently active eolian dunes, but do not show dominant provenance affinity with modern Indus River sediment, we infer that modern dune activity in that part of the desert reworks chiefly older Indus and Nara fluvial sediment (cf. statistical similarity between UN1, Nara, and mid-Holocene and LGM Indus samples; Fig. 3B). Because the U-Pb zircon ages in the sample from active dune sand at NM3 differed from those of any other sample, there may be an additional sediment source at or upwind of NM3 that we have not identified.

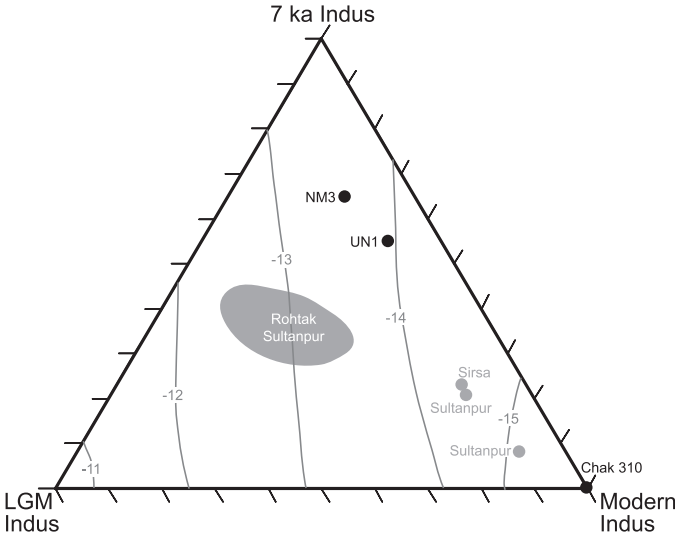

FIG. 5.—Ternary diagram showing possible mixing relationships among different compositions of the mainstem Indus River–delta region at three time periods: the last glacial maximum (LGM), 7 ka, and modern time. Black dots show the estimated contributions of Indus sediment of these three ages in three Thar Desert dune samples based on zircon age spectra, whereas gray contours show the ε_{Nd} values that would be associated with these mixtures. Gray shaded regions indicate estimates for sediments for which only Nd isotope data (but not zircon data) are available. See text and Table 3 for data sources.

The northeastern portion of the Thar Desert apparently had a somewhat different provenance history than we have inferred for either the northwestern (Cholistan) region or the southern region around sites NM3 and UN1. Although no zircon data are available from the northeastern desert, we can compare their Nd isotope compositions against Nd isotope compositions known for the Indus sediment sources of three time periods (gray contours and shaded regions in Fig. 5). This allows us to compare sediments with only zircon data to those constrained only by Nd isotopes, even if there is less certainty about where in the ternary plot the Nd-based samples would place precisely.

The ε_{Nd} patterns at Rohtak and Sultanpur (Tripathi et al. 2004) were generally less negative than the –14.5 value obtained from an eolian dune at Yazman, in Cholistan (Fig. 4), although some of the dunes also show more negative values, implying either greater input from the modern Indus delta (similar to Chak-310) or possibly sediment contributions from local rivers such as the Sutlej River or possibly the Yamuna River before its capture away from the Indus basin (before 10 ka; Clift et al. 2012). ε_{Nd} values of eolian dune sand in the range –12 to –14 suggest some influx of LGM-age Indus delta material (ε_{Nd} –10.8; Figs. 4, 5); the Indus delta has had ε_{Nd} values of –13 or less since ~ 8 ka (Clift et al. 2008). The range of ε_{Nd} values in eolian sand from the northeastern part of the desert overlaps with those of the Punjabi floodplain material, as well as mainstem Indus sediment of ages ranging from LGM to modern (Fig. 4). It is not practical to separate the contributions from modern mainstem Indus (far-field eolian) and Punjabi floodplain (local eolian) sources because their ε_{Nd} values are quite similar (Fig. 4), and there could be substantial exchange of fluvial and eolian sediment locally. LGM-age Indus sediment could have contributed as much as 60% (relative to modern Indus or local Punjabi floodplain sources) to generate those ε_{Nd} values at the least-negative end of the Thar Desert range (–12.6; Figs. 4, 5). The range of Nd isotope values in the northeastern desert suggests that any eolian reworking of LGM-age sediment from the Indus delta into that region either was limited in volume or was diluted subsequently by isotopically more negative sediments (Fig. 4).

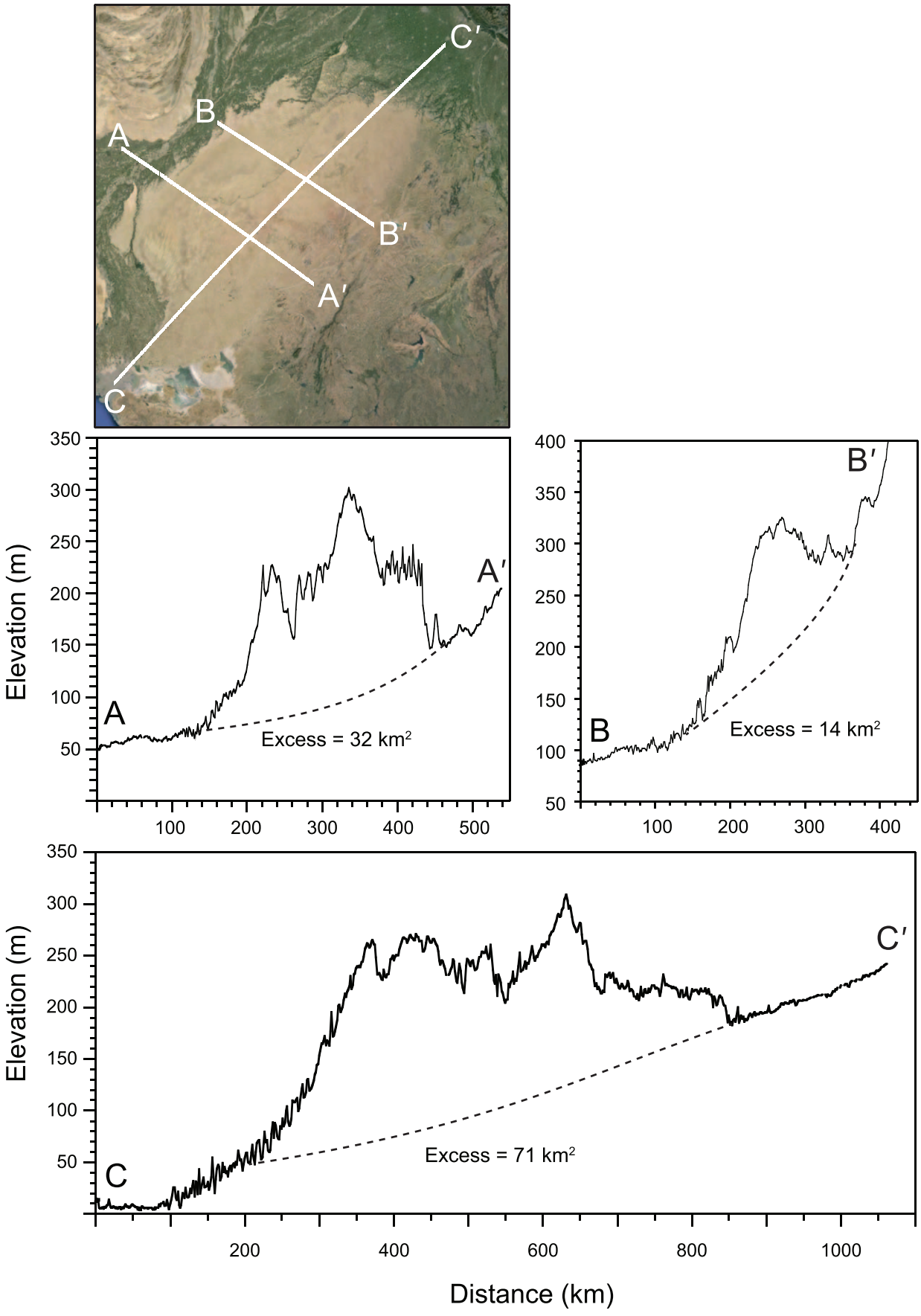
A
A′
B
B′
C
C′
Elevation (m)
Excess = 32 km²
Excess = 14 km²
Excess = 71 km²
Distance (km)

Finally, we consider storage of Indus River material in the Thar Desert in the context of the large Indus basin sediment-routing system. The lower Indus River and delta region likely has provided sediment to Thar Desert eolian dunes since ~ 8 ka (e.g., Gupta et al. 2003), when the desert expanded westward to directly adjoin the mainstem Indus course on the upwind side, and possibly since the mid-Pleistocene (Singvi et al. 2010), although we have not investigated paleodune composition. The provenance signal of the lower Indus River dominates at least some areas of the downwind end of the desert, indicating that far-field eolian delivery is an important sediment-transport process in this system, such that almost all of the eolian sand in at least parts of the Thar Desert could be derived from far-field Indus River sources (based on our mixing calculations for the Chak-310 site). Thus, we consider the importance of sediment storage in the Thar Desert from a volumetric standpoint relative to other sedimentary buffers in the Indus basin.

To estimate the total sediment volume in the Thar Desert, we evaluated the topographic anomaly of the desert compared to the long-wavelength sloping topography of the Indus drainage basin, using Shuttle Radar Topography Mission (SRTM) data (Fig. 6). The land-surface elevation in the desert is somewhat higher than that which would be inferred from an extrapolation of the Indus basin topography on either side of the desert, and cross sections through this elevated region can be used to infer the total sediment volume in the desert. A minimum estimate can be obtained by treating the desert as a simple cone of sand 200 m high with a radius of 150 km, which would indicate a volume of 4700 km^3. This ignores thinner sediments in the northern region of the desert, which extends> 600 km along its NE–SW axis (Fig. 6). However, if we treat the NE–SW profile (C–C′ in Fig. 6) as being a representative cross section along the crest of the desert sediment accumulation and extending across a width of 300 km, then we would estimate a total volume of ~ 10,600 km^3, assuming that the desert sediment accumulation has a tapering triangular cross section. To be as conservative as possible, we favor the lower estimate of 4700 km^3. Such a sediment volume is geologically reasonable, given the distribution and size of individual sand dunes in the Thar Desert, although likely an underestimate of the total sediment volume. Given that Thar Desert linear dunes commonly measure 2–4 km long by 0.15–0.25 km wide by 5–10 m tall in Google Earth^{TM} aerial imagery, and that the transverse and parabolic dunes commonly measure 1–3 km wide by 0.5–0.8 km long by 15–25 m tall, on the order of a hundred thousand dunes of such size can account for a sand volume of 4700 km^3. Therefore, this seems a reasonable, if low, volume estimate for the Thar Desert; our volume estimate is especially conservative given that these latter calculations account only for sediment in dunes, and ignore interdune sediment and loess deposits (e.g., in the Chundkho section; Fig. 2), as well as developed and irrigated regions without modern dune forms. However, recycling of desert sediment into the Indus River system will be most important in the western and northern regions of the Thar Desert (where fluvial channels drain to the Indus River), so that the entire desert sediment volume would not be involved in the buffering effect we describe—not all Thar Desert sediment will ultimately cycle downwind into fluvial channels that join the Indus. Eolian sediment blowing into the eastern part of the desert could, presumably, leave the Indus watershed altogether and supply sediment into the Ganges basin or the Kutch region (note eastern boundary of the Indus watershed on Fig. 1A), making the Thar Desert a ''leaky sink'' for sediment storage.

Volumetrically, then, the Thar Desert stores three orders of magnitude less sediment than does the Indus submarine fan (4,700 km^3 vs. 5,000,000 km^3; Naini and Kolla 1982). Although the desert is a minor sediment sink compared to the ultimate marine sink, the desert stores a greater sediment volume than all other known sediment-storage locales in the Indus Basin combined (Figs. 7, 8). The desert represents a much larger sediment sink, for example, than does sediment storage in Himalayan valley fills of the Indus basin headwaters (~ 250–270 km^3; Blöthe and Korup 2013; Clift and Giosan, 2014). Lag times also could be substantially longer for sediment in the Thar Desert, perhaps as long as 10^6 yr (cf. Vermeesch et al. 2010), whereas Himalayan valley fill has sediment residence times of 10^3–10^5 yr (Blöthe and Korup 2013)—although the inference of modern Indus-composition sand in Cholistan suggests residence times in the Thar Desert could be as short as 10^3 yr. The sediment volume in the Thar Desert is also at least twice as large as the sediment volume deposited since the LGM in the largest alluvial segment of the mainstem Indus River (725–2500 km^3 in the Sindh alluvial plain; Clift and Giosan 2014). Therefore, we conclude that eolian transport of river material into temporary storage in the desert introduces a volumetrically and probably temporally important buffer to the sediment-transfer zone. It is likely that fluvial–eolian interactions affect sediment routing in other dryland systems as well, but that this process has not been widely recognized. Although the Thar Desert is inferred to be a substantial buffer of

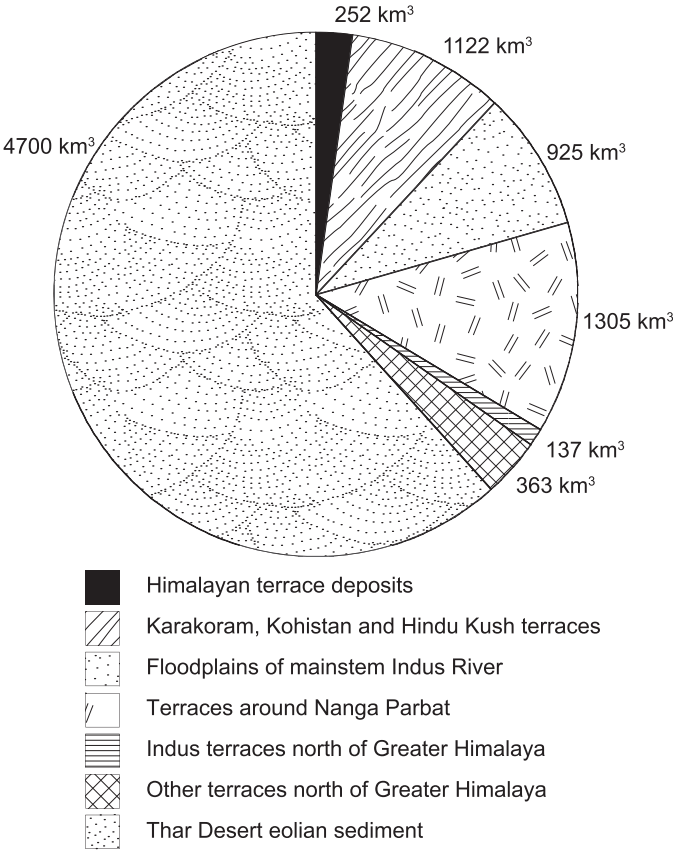

FIG. 7.—Relative proportions of sediment stored in the Thar Desert (from a conservative volume estimate; see text) compared to other temporary sediment stores in the Indus basin, all of which have contributed reworked sediment to the Indus delta since the last glacial maximum (LGM; Clift and Giosan 2014). Terrace deposits in mountainous regions include both fluvial deposits and lesser volumes of mass-wasted material (Blöthe and Korup 2013).

←

FIG. 6.—Topographic profiles across the Thar Desert, from Shuttle Radar Topography Mission (SRTM) data (www.geomapapp.org), showing the mounding of desert topography over a regional slope for this part of the Indus basin, inferred as shown by the dashed lines. Topography above the dashed line is assumed to represent desert sediment.

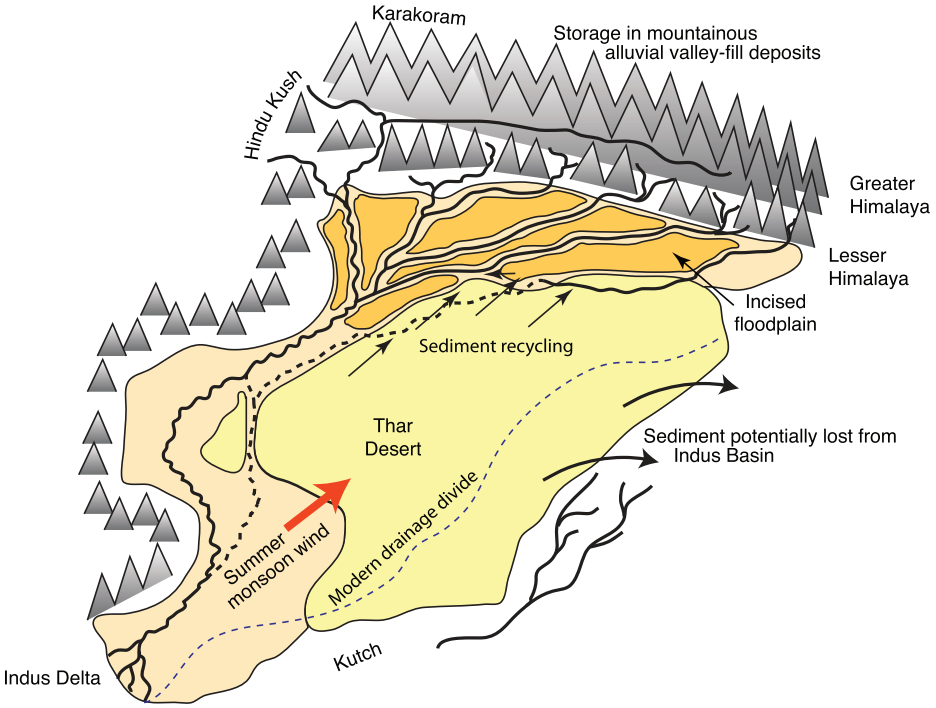

FIG. 8.—Schematic representation of sediment routing in the Indus basin and surrounding region. Refer to Figure 7 for several temporary sediment sinks in mountainous regions that are not apparent at the larger scale of this diagram.

sediment being transported toward the Arabian Sea, this process is likely variable through geologic time. Northeastward eolian sediment-transport potential is presumably greatest during times when the summer monsoon winds are strong, such as during the mid-Holocene (11–6 ka; Sirocko et al. 1996). In contrast, the last glacial episode was characterized by weaker summer monsoon winds and, we surmise, probably less eolian sediment recycling.

CONCLUSIONS

Isotopic similarities between Indus River fluvial sediment and Thar Desert eolian sediment indicate that most of the sediment in the sampled desert regions is derived from wind-reworked fluvial deposits of the lower Indus River and delta. Sediment storage in the desert thus can be considered to buffer, or delay, sediment transfer from the Himalayas to the Indus submarine fan, potentially affecting transmission of environmental signals to the marine stratigraphic record. Although sediment storage in the Thar Desert is volumetrically small relative to the marine sedimentary sink (the Indus fan), it is important to recognize fluvial–eolian cycling as a process that can interrupt the transfer of sediment-flux signals to the marine record, for at least a small proportion of the sediment in the Indus transfer system. The sediment volume stored in the desert is inferred to be ~ 18 times greater than that of alluvial and mass-wasting deposits that store sediment in the Himalayan headwater regions of the Indus basin, is at least twice as great as the largest alluvial-plain segment of the mainstem Indus River, and is greater than the combined volume of all other known sediment buffer zones in the Indus sediment-routing system. Residence times of Indus sediment in the Thar Desert are likely comparable to or longer than lag times in alluvial buffering systems. The importance of this recycling between the fluvial and eolian system must vary through time depending on the size of the desert, the transport capacity of summer monsoon winds, and sediment supply from the Himalaya, all of which are linked to monsoon intensity and in turn to glacial–interglacial cycles.

SUPPLEMENTAL MATERIAL

A table with analyses from new samples is available from JSR's Data Archive: http://sepm.org/pages.aspx?pageid=229.

ACKNOWLEDGMENTS

PDC thanks the Charles T. McCord chair fund at LSU for assistance in undertaking this work. The authors thank L. Giosan for valuable discussions. J.K. Tripathi kindly provided quantitative Nd isotope data that were not explicitly presented by Tripathi et al. (2004). E. Hajek, R. Wasson, and J. Warrick provided insightful and constructive review comments that improved the manuscript. We thank J. Gillies, J. MacEachern, and J.B. Southard for their editorial work.

REFERENCES

ALIZAI, A., CLIFT, P.D., GIOSAN, L., VANLANINGHAM, S., HINTON, R., TABREZ, A.R., DANISH, M., AND EIMF, 2011a, Pb isotopic variability in the modern and Holocene Indus River system measured by ion microprobe in detrital K-feldspar grains: Geochimica et Cosmochimica Acta, v. 75, p. 4771–4795.

ALIZAI, A., CARTER, A., CLIFT, P.D., VANLANINGHAM, S., WILLIAMS, J.C., AND KUMAR, R., 2011b, Sediment provenance, reworking and transport processes in the Indus River by U–Pb dating of detrital zircon grains: Global and Planetary Change, v. 76, p. 33–55.

AMIDON, W.H., BURBANK, D.W., AND GEHRELS, G.E., 2005, Construction of detrital mineral populations: insights from mixing of U-Pb zircon ages in Himalayan rivers: Basin Research, v. 17, p. 463–485.

AMIT, R., ENZEL, Y., CROUVI, O., SIMHAI, O., MATMON, A., PORAT, N., MCDONALD, E., AND GILLESPIE, A.R., 2011, The role of the Nile in initiating a massive dust influx to the Negev late in the middle Pleistocene: Geological Society of America, Bulletin, v. 123, p. 873–889.

ARMITAGE, J.J., JONES, T.D., DULLER, R.A., WHITTAKER, A.C., AND ALLEN, P.A., 2013, Temporal buffering of climate-driven sediment flux cycles by transient catchment response: Earth and Planetary Science Letters, v. 369–370, p. 200–210.

BELNAP, J., MUNSON, S.M., AND FIELD, J.P., 2011, Aeolian and fluvial processes in dryland regions: the need for integrated studies: Ecohydrology, v. 4, p. 615–622.

BLACK, L.P., KAMO, S.L., ALLEN, C.M., ALEINIKOFF, J.N., DAVIS, D.W., KORSCH, R.J., AND FOUDOULIS, C., 2003, TEMORA 1: a new zircon standard for Phanerozoic U–Pb geochronology: Chemical Geology, v. 200, p. 155–170.

Blöthe, J.H., and Korup, O., 2013, Millennial lag times in the Himalayan sediment routing system: Earth and Planetary Science Letters, v. 382, p. 38–46.
Bracken, L.J., Turnbull, L., Wainwright, J., and Bogaart, P., 2015, Sediment connectivity: a framework for understanding sediment transfer at multiple scales: Earth Surface Processes and Landforms, v. 40, p. 177–188.
Bullard, J.E., and Livingstone, I., 2002, Interactions between aeolian and fluvial systems in dryland environments: Area, v. 34.1, p. 8–16.
Bullard, J.E., and McTainsh, G.H., 2003, Aeolian–fluvial interactions in dryland environments: examples, concepts, and Australia case study: Progress in Physical Geography, v. 27, p. 471–501.
Carter, A., and Bristow, C.S., 2001, Detrital zircon geochronology: enhancing the quality of sedimentary source information through improved methodology and combined U–Pb and fission-track techniques: Basin Research, v. 12, p. 47–57.
Castelltort, S., and Van Den Driessche, J., 2003, How plausible are high-frequency sediment supply-driven cycles in the stratigraphic record?: Sedimentary Geology, v. 157, p. 3–13.
Clift, P.D., and Giosan, L., 2014, Sediment fluxes and buffering in the post-glacial Indus Basin: Basin Research, v. 26, p. 369–386.
Clift, P.D., Lee, J.I., Hildebrand, P., Shimizu, N., Layne, G.D., Blusztajn, J., Blum, J.D., Garzanti, E., and Khan, A.A., 2002, Nd and Pb isotope variability in the Indus River system: implications for sediment provenance and crustal heterogeneity in the western Himalaya: Earth and Planetary Science Letters, v. 200, p. 91–106.
Clift, P.D., Campbell, I.H., Pringle, M.S., Carter, A., Zhang, X., Hodges, K.V., Khan, A.A., and Allen, C.M., 2004, Thermochronology of the modern Indus River bedload: new insight into the control on the marine stratigraphic record: Tectonics, v. 23, TC5013.
Clift, P.D., Giosan, L., Blusztajn, J., Campbell, I.H., Allen, C., Pringle, M., Tabrez, A.R., Danish, M., Rabbani, M.M., Alizai, A., Carter, A., and Lückge, A., 2008, Holocene erosion of the Lesser Himalaya triggered by intensified summer monsoon: Geology, v. 36, p. 79–82.
Clift, P.D., Carter, A., Giosan, L., Durcan, J., Tabrez, A.R., Alizai, A., VanLaningham, S., Duller, G.A.T., Macklin, M.G., Fuller, D.Q., and Danish, M., 2012, U-Pb zircon dating evidence for a Pleistocene Sarasvati River and Capture of the Yamuna River: Geology, v. 40, p. 212–215.
Decelles, P.G., Gehrels, G.E., Quade, J., Lareau, B., and Spurlin, M., 2000, Tectonic implications of U-Pb zircon ages of the Himalayan orogenic belt in Nepal: Science, v. 288, p. 497–499.
Depaolo, D.J., and Wasserburg, G.J., 1976, Nd isotopic variations and petrogenetic models: Geophysical Research Letters, v. 3, p. 249–252.
Draut, A.E., 2012, Effects of river regulation on aeolian landscapes, Colorado River, southwestern USA: Journal of Geophysical Research, v. 117, F2022.
Dunne, T., Mertes, L.A.K., Meade, R.H., Richey, J.E., and Forsberg, B.R., 1998, Exchanges of sediment between the flood plain and channel of the Amazon River in Brazil: Geological Society of America, Bulletin, v. 110, p. 450–467.
Durcan, J.A., Roberts, H.M., Duller, G.A.T., and Alizai, A.H., 2010, Testing the use of range-finder OSL dating to inform field sampling and laboratory processing strategies: Quaternary Geochronology, v. 5, p. 86–90.
Enzel, Y., Ely, L.L., Mishra, S., Ramesh, R., Amit, R., Lazar, B., Rajaguru, S.N., Baker, V.R., and Sandler, A., 1999, High-resolution Holocene environmental changes in the Thar Desert, northwestern India: Science, v. 284, p. 125–128.
Fleitmann, D., Burns, S.J., Mudelsee, M., Neff, U., Kramers, J., Mangini, A., and Matter, A., 2003, Holocene forcing of the Indian monsoon recorded in a stalagmite from southern Oman: Science, v. 300, p. 1737–1739.
Forzoni, A., Storms, J.E.A., Whittaker, A.C., and de Jager, G., 2014, Delayed delivery from the sediment factory: modeling the impact of catchment response time to tectonics on sediment flux and fluvio-deltaic stratigraphy: Earth Surface Processes and Landforms, v. 39, p. 689–704.
Fraser, J.E., Searle, M.P., Parrish, R.R., and Noble, S.R., 2001, Chronology of deformation, metamorphism, and magmatism in the southern Karakoram Mountains: Geological Society of America, Bulletin, v. 113, p. 1443–1455.
Gehrels, G.E., Decelles, P.G., Ojha, T.P., and Upreti, B.N., 2006, Geologic and U-Th-Pb geochronologic evidence for early Paleozoic tectonism in the Kathmandu thrust sheet, central Nepal Himalaya: Geological Society of America, Bulletin, v. 118, p. 185–198.
Gibling, M.R., Sinha, R., Roy, N.G., Tandon, S.K., and Jain, M., 2008, Quaternary fluvial and eolian deposits on the Belan river, India: paleoclimatic setting of Paleolithic to Neolithic archeological sites over the past 85,000 years: Quaternary Science Reviews, v. 27, p. 391–410.
Giosan, L., Clift, P.D., Macklin, M.G., Fuller, D.Q., Constantinescu, S., Durcan, J.A., Stevens, T., Duller, G.A.T., Tabrez, A., Adhikari, R., Gangal, K., Alizai, A., Filip, F., VanLaningham, S., and Syvitski, J.P.M., 2012, Fluvial landscapes of the Harappan civilization: National Academy of Sciences [USA], Proceedings, v. 109, p. 1688–1694.
Glennie, K.W., Singhvi, A.K., Lancaster, N., and Teller, J.T., 2002, Quaternary climatic changes over Southern Arabia and the Thar Desert, India, *in* Clift, P.D., Kroon, D., Gaedicke, C., and Craig, J., eds., The Tectonic and Climatic Evolution of the Arabian Sea Region: Geological Society of London, Special Publication 195, p. 301–316.
Goodbred, S.L., 2003, Response of the Ganges dispersal system to climate change: a source-to-sink view since the last interstade: Sedimentary Geology, v. 162, p. 83–103.
Gupta, A.K., Anderson, D.M., and Overpeck, J.T., 2003, Abrupt changes in the Asian southwest monsoon during the Holocene and their links to the North Atlantic Ocean: Nature, v. 421, p. 354–356.
Han, G., Zhang, G., and Dong, Y., 2007, A model for the active origin and development of source-bordering dunefields on a semiarid fluvial plan: a case study from the Xiliaohe Plain, Northeast China: Geomorphology, v. 86, p. 512–524.
Hodges, K.V., Parrish, R.R., and Searle, M.P., 1996, Tectonic evolution of the central Annapurna Range, Nepalese Himalayas: Tectonics, v. 15, p. 1264–1291.
Kameswara Rao, K., Wasson, R.J., and Kutty, M.K., 1989, Foraminifera from late Quaternary dune sands of the Thar Desert, India: Palaios, v. 4, p. 168–180.
Kar, A., 1993, Aeolian processes and bedforms in the Thar desert: Journal of Arid Environments, v. 25, p. 83–96.
Le Fort, P., Debon, F., and Sonet, J., 1983, Petrography, geochemistry, and geochronology of some samples from the Karakoram Batholith (N. Pakistan), *in* Shams, F.A., ed., Granites of the Himalayas, Karakoram and Hindu Kush: Lahore, Pakistan, Punjab University, p. 377–387.
Muhs, D.R., Reynolds, R.L., Been, J., and Skipp, G., 2003, Eolian sand transport pathways in the southwestern United States: importance of the Colorado River and local sources: Quaternary International, v. 104, p. 3–18.
Naini, B.R., and Kolla, V., 1982, Acoustic character and thickness of sediments of the Indus Fan and the continental margin of western India: Marine Geology, v. 47, p. 181–185.
Noble, S.R., and Searle, M.P., 1995, Age of crustal melting and leucogranite formation from U-Pb zircon and monazite dating in the western Himalaya, Zanskar, India: Geology, v. 23, p. 1135–1138.
Parrish, R.R., and Hodges, K.V., 1996, Isotopic constraints on the age and provenance of the Lesser and Greater Himalayan sequences, Nepalese Himalaya: Geological Society of America, Bulletin, v. 108, p. 904–911.
Parrish, R.R., and Tirrul, R., 1989, U-Pb age of the Baltoro Granite, Northwest Himalaya, and implications for monazite U-Pb systematics: Geology, v. 17, p. 1076–1079.
Pearce, N.J.G., Perkins, W.T., Westgate, J.A., Gorton, M.P., Jackson, S.E., Neal, C.R., and Chenery, S.P., 1997, A compilation of new and published major and trace element data for NIST SRM 610 and NIST SRM 612 glass reference materials: Geostandards Newsletter, v. 21, p. 115–144.
Petter, A.L., Steel, R.J., Mohrig, D., Kim, W., and Carvajal, C., 2013, Estimation of the paleoflux of terrestrial-derived solids across ancient basin margins using the stratigraphic record: Geological Society of America, Bulletin, v. 125, p. 578–593.
Pizzuto, J.E., 2014, Long-term storage and transport length scale of fine sediment: analysis of a mercury release into a river: Geophysical Research Letters, v. 41, p. 5875–5882.
Prins, M.A., Zheng, H., Beets, K., Troelstra, S., Bacon, P., Kamerling, I., Wester, W., Konert, M., Huang, X., Ke, W., and Vandenberghe, J., 2009, Dust supply from river floodplains: the case of the lower Huang He (Yellow River) recorded in a loess–palaeosol sequence from the Mangshan Plateau: Journal of Quaternary Science, v. 24, p. 75–84.
Ramsey, M.S., Christensen, P.R., Lancaster, N., and Howard, D.A., 1999, Identification of sand sources and transport pathways at the Kelso Dunes, California, using thermal infrared remote sensing: Geological Society of America, Bulletin, v. 111, p. 646–662.
Reimer, P.J., Baillie, M.G.L., Bard, E., Bayliss, A., Beck, J.W., Bertrand, C.J.H., Blackwell, P.G., Buck, C.E., Burr, G.S., Cutler, K.B., Damon, P.E., Edwards, R.L., Fairbanks, R.G., Friedrich, M., Guilderson, T.P., Hogg, A.G., Hughen, K.A., Kromer, B., McCormac, G., Manning, S., Ramsey, C.B., Reimer, R.W., Remmele, S., Southon, J.R., Stuiver, M., Talamo, S., Taylor, F.W., van der Plicht, J., and Weyhenmeyer, C.E., 2004, IntCal04 terrestrial radiocarbon age calibration, 0–26 cal kyr BP: Radiocarbon, v. 46, p. 1029–1058.
Roskin, J., Katra, I., Agha, N., Goring-Morris, A.N., Porat, N., and Barzilai, O., 2014, Rapid anthropogenic response to short-term aeolian–fluvial palaeoenvironmental changes during the Late Pleistocene–Holocene transition in the northern Negev Desert, Israel: Quaternary Science Reviews, v. 99, p. 176–192.
Saini, H.S., Tandon, S.K., Mujtaba, S.A.I., Pant, N.C., and Khorana, R.K., 2009, Reconstruction of buried channel-floodplain systems of the northwestern Haryana Plains and their relation to the "Vedic" Saraswati: Current Science, v. 97, p. 1634–1643.
Schärer, U., Copeland, P., Harrison, T.M., and Searle, M.P., 1990, Age, cooling history, and origin of post-collisional leucogranites in the Karakoram Batholith; a multi-system isotope study: Journal of Geology, v. 98, p. 233–251.
Searle, M.P., Parrish, R.R., Tirrul, R., and Rex, D.C., 1990, Age of crystallization of the K2 gneiss in the Baltoro Karakoram: Geological Society of London, Journal, v. 147, p. 603–606.
Simpson, G., and Castelltort, S., 2012, Model shows that rivers transmit high-frequency climate cycles to the sedimentary record: Geology, v. 40, p. 1131–1134.
Singhvi, A.K., and Kar, A., 2004, The aeolian sedimentation record of the Thar desert: Indian Academy of Sciences, Proceedings, v. 113, p. 371–401.
Singhvi, A.K., Williams, M.A.J., Rajaguru, S.N., Misra, V.N., Chawla, S., Stokes, S., Chauhan, N., Francis, T., Ganjoo, R.K., and Humphreys, G.S., 2010, A 200 ka record of climatic change and dune activity in the Thar Desert, India: Quaternary Science Reviews, v. 29, p. 3095–3105.
Sirocko, F., Garbe-Schönberg, D., McIntyre, A., and Molfino, B., 1996, Teleconnections between the subtropical monsoons and high-latitude climates during the last deglaciation: Science, v. 272, p. 526–529.
Sláma, J., Kosler, J., Condon, D.J., et al. (2008), 2008, Plezovice zircon: a new natural reference material for U–Pb and Hf isotopic microanalysis: Chemical Geology, v. 249, p. 1–35.

Stuiver, M., Reimer, P.J., Bard, E., Beck, J.W., Burr, K.A., Hughen, K.A., Kromer, B., McCormac, J., van der Plicht, J., and Spurk, M., 1998, INTCAL98 radiocarbon age calibration: Radiocarbon, v. 40, p. 1041–1083.

Tanaka, T., Togashi, S., Kamioka, H., Amakawa, H., Kagami, H., Hamamoto, T., Yuhara, M., Orihashi, Y., Yoneda, S., Shimizu, H., Kunimaru, T., Takahashi, K., Yanagi, T., Nakano, T., Fujimaki, H., Shinjo, R., Asahara, Y., Tanimizu, M., and Dragusanu, C., 2000, JNdi-1: a neodymium isotopic reference in consistency with La Jolla neodymium: Chemical Geology, v. 168, p. 279–281.

Trimble, S.W., 1983, A sediment budget for Coon Creek basin in the Driftless Area, Wisconsin, 1853–1977: American Journal of Science, v. 283, p. 454–474.

Tripathi, J.K., Bock, B., Rajamani, V., and Eisenhauer, A., 2004, Is River Ghaggur, Saraswati? Geochemical constraints: Current Science, v. 87, p. 1141–1145.

Valdiya, K.S., 2002, Saraswati: the River that Disappeared: Hyderabad, India, 1st University Press, 116 p.

Vermeesch, P., 2013, Multi-sample comparison of detrital age distributions: Chemical Geology, v. 341, p. 140–146.

Vermeesch, P., 2004, How many grains are needed for a provenance study?: Earth and Planetary Science Letters, v. 224, p. 351–441.

Vermeesch, P., Fenton, C.R., Kober, F., Wiggs, G.F.S., Bristow, C.S., and Xu, S., 2010, Sand residence times of one million years in the Namib Sand Sea from cosmogenic nuclides: Nature Geoscience, v. 3, p. 862–865.

Wasson, R.J., Rajaguru, S.N., Misra, V.N., Agrawal, D.P., Dhir, R.P., Singhvi, A.K., and Kameswara Rao, K., 1983, Geomorphology, late Quaternary stratigraphy, and paleoclimatology of the Thar dune field: Zeitschrift für Geomorphologie, Supplement Volumes, v. 45, p. 117–151.

Wiedenbeck, M., Hanchar, J.M., Peck, W.H., Sylvester, P., Valley, J., Whitehouse, M., Kronz, A., Morishita, Y., Nasdala, L., Fiebig, J., Franchi, I., Girard, J.-P., Greenwood, R.C., Hinton, R., Kita, N., Mason, P.R.D., Norman, M., Ogasawara, M., Piccoli, P.M., Rhede, D., Satoh, H., Schulz-Dobrick, B., Skår, O., Spicuzza, M.J., Terada, K., Tindle, A., Togashi, S., Vennemann, T., Xie, Q., and Zhen, Y.-F., 2004, Further characterization of the 91500 zircon crystal: Geostandards and Geoanalytical Research, v. 28, p. 9–39.

Wolinsky, M.A., Swenson, J.B., Litchfield, N., and McNinch, J.E., 2010, Coastal progradation and sediment partitioning in the Holocene Waipaoa sedimentary system, New Zealand: Marine Geology, v. 270, p. 94–107.

Yang, S., Zhang, F., and Wang, Z., 2012., Grain size distribution and age population of detrital zircons from the Changjiang (Yangtze) River system, China: Chemical Geology, v. 296–297, p. 26–38.

Received 17 November 2014; accepted 9 March 2015.